Optik 123 (2012) 1742–1745

Contents lists available at SciVerse ScienceDirect

Optik

journal homepage: www.elsevier.de/ijleo

# Dynamic phase profile of phase objects based in the use of a quasi-common path interferometer

David Ignacio Serrano-García[a,*], Noel Ivan Toto-Arellano[a,b,c,*], Amalia Martínez-García[a], Juan Antonio Rayas Álvarez[a], Gustavo Rodríguez Zurita[b]

[a] Centro de Investigaciones en Óptica, A.C., León, Gto, Mexico
[b] Laboratorio de Óptica Física de la Benemérita Universidad Autónoma de Puebla, Pue, Mexico
[c] Universidad Tecnológica de Tulancingo, Tulancingo, Hidalgo, Mexico

ARTICLE INFO

*Article history:*
Received 27 November 2011
Accepted 27 February 2012

*Keywords:*
Phase shifting
Interferometry
Grating
Polarization

ABSTRACT

In this paper, we propose a quasi common-path interferometer based on a two beams configuration (TBC) using simultaneous phase shifting interferometry modulated by polarization that shows insensitivity against external vibration. Due to the fact that the configuration is capable of obtaining two beams whose separation can be varied, according to the characteristics of the grid used, to obtain the interference patterns. It can be used to implement a quasi-common path interferometer that allows the measurement of dynamic events with high accuracy. For demodulate the fringe patterns generated by the optical system we using the conventional four step phase shifting method. Experimental results are also given.



## 1. Introduction

In this paper, we propose a quasi common path interferometer using polarizing phase shifting interferometry [1–3]. Currently, phase-shifting techniques for polarization are being applied in various areas such as, digital holography [4–6], ESPI and shearography [7–11] because they allow non-invasive analysis of the samples. The use of phase shifting modulated by polarization has the advantage of not requiring mechanical components, such as PZT, to obtain the phase shifts, decreasing the sensibility of the system against external vibrations. The developed system is capable of obtain two beams with adjustable separation, this allows the two beams move in the $x$-axis or $y$-axis, for convenience; it can be used to implement a quasi-common path interferometer that allows the measurement of phase profiled of transparent samples. The optical set-up proposed use conventional lineal polarizers placed at conventional angles presenting the advantage of not require micro-polarizer's arrays [12,13] and the interferometer is stable to external vibrations. Unlike previously proposed interferometers, this system does not use a conventional double window; it generates two beams whose separation can be varied according to the characteristics of the phase grid used for generated 2D interference patterns. Experimental results for phase objects are also presented.

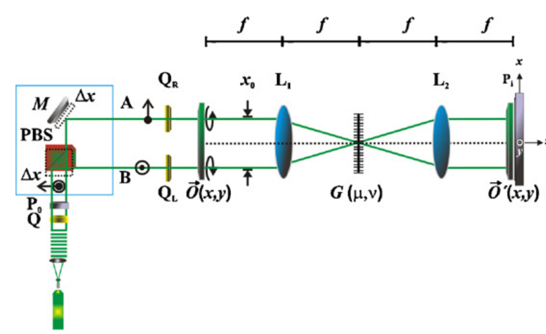


**Fig. 1.** Quasi common path interferometer. $M$: mirror; PBS: polarizing beam splitter; $O(x, y)$: object plane; $O'(x, y)$: image plane; $L_i$: lens; $G(\mu,\nu)$: phase grid; $P_i$: polarizers; $Q_i$: quarter wave plates.

## 2. Experimental set-up

Fig. 1 shows the experimental set-up used. A linear polarizing filter ($P_0$) generates linearly polarized light oriented to 45° entering in the arrangement shown in Fig. 1 enclosed a rectangle, from a $YVO_3$ laser operating at 532 nm. This set-up generates two displaced beams by moving a same distance $\Delta x$ to mirror $M$ and the polarizing beam splitter (PBS), enabling one to change the spacing $x_0$ between beams centres. The presented system

* Corresponding authors at: Centro de Investigaciones en Óptica, A.C., León, Gto, Mexico. Tel.: +55 294 9422796.
*E-mail addresses:* david@cio.mx (D.I. Serrano-García), ivantotoarellano@hotmail.com (N.I. Toto-Arellano).

0030-4026/$ – see front matter © 2012 Elsevier GmbH. All rights reserved.
http://dx.doi.org/10.1016/j.ijleo.2012.02.044

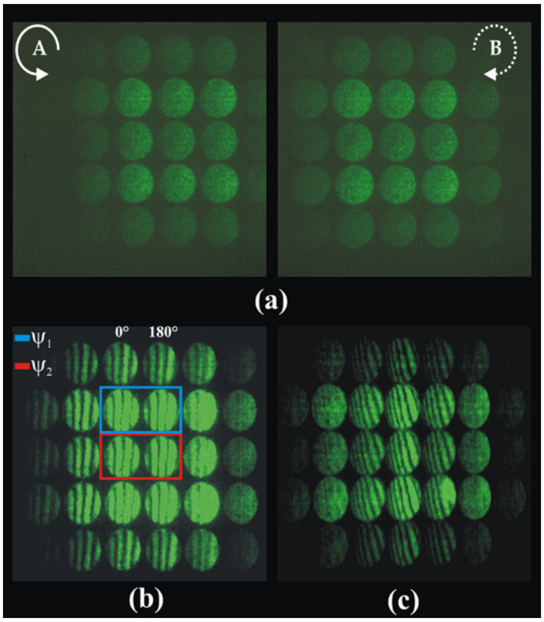


**Fig. 2.** (a) Replicas in the image plane for each beams, (b) resultant interference patterns, from beam separation of $x_0$ = 0.8 cm, (c) by changing beam separation, we can properly interfere different order diffractions, for $x_0$ = 1.8 cm.

simplifies other arrangements, which is coupled a Mach Zehnder interferometer or Cyclic Shear interferometer to generate a double window, making it more stable to external vibrations. In order to generate cross circular polarization beams, we place a quarter wave plate ($Q$) on each beam, $Q_L$ and $Q_R$ placed in the path of beam $A$ and $B$ respectively. The system is coupled to 4-$f$ arrangement using two similar achromatic lenses of focal length $f$ = 20 cm and a phase grid $G(\mu,\nu)$ placed as the system's pupil with frequency $d$ = 110 ln/mm. In the phase grid used, $\mu = u/\lambda f$ and $\nu = v/\lambda f$ are the frequency coordinates $(u,v)$ scaled to wavelength $\lambda$ and focal length $f$.

Diffraction orders appear on the image plane, forming a rectangular array. Around each order, an interference pattern appears due to the optical fields associated to each beam when proper matching conditions are met. The interference patterns arise due to the superposition of the diffraction patterns generated by each beam. The resulting centered phase grid can be written as

$$G(\mu, \upsilon) = \sum_{q=-\infty}^{\infty} J_q(2\pi A_g) e^{i2\pi \cdot qX_0\mu} \sum_{r=-\infty}^{\infty} J_r(2\pi A_g) e^{i2\pi \cdot rX_0\upsilon} \quad (1)$$

with $2\pi A_g$ being the grating phase amplitude, and $J_q$ and $J_r$ the Bessel functions of the first kind of integer order $q$, $r$ respectively. $X_0$ is the separation of two neighbouring diffraction orders in the image plane. The Fourier transform of the phase grid becomes

$$\tilde{G}(x, y) = \sum_{q=-\infty}^{q=\infty} \sum_{r=-\infty}^{r=\infty} J_q(2\pi A_g)\ J_r(2\pi A_g)\ \ \delta(x - qX_0,\ y - rX_0) \quad (2)$$

## 3. Polarizing phase shifting grid interferometry

Phase grid interferometry is based on a two crossed phase grating placed as the pupil in a 4-$f$ Fourier optical system. A convenient

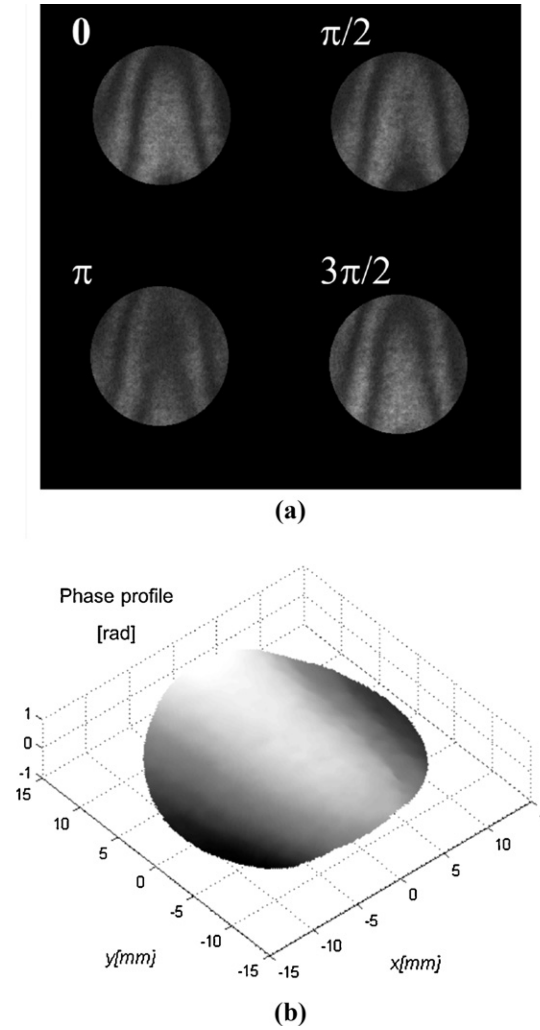


**Fig. 3.** Platform based on a Labview used to automatize the interferograms capture and phase processing. (a) Interference patterns, (b) phase profile of the phase object.

beam pair for a grating interferometer implies a vectorial amplitude transmittance given by

$$\vec{O}(x, y) = \vec{J}_L \cdot A\left(x + \frac{x_0}{2}, y\right) + \vec{J}_R B\left(x - \frac{x_0}{2}, y\right) \quad (3)$$

where $x_0$ is considered as the mutual separations between the centres of each beam along the coordinate axis, with an arbitrary retardation $\alpha' = 1.519$ rad and the Jones vectors, $\vec{J}_L$ and $\vec{J}_R$, defined as

$$\vec{J}_L = \begin{pmatrix} 1 \\ e^{i\alpha'} \end{pmatrix}, \quad \vec{J}_R = \begin{pmatrix} 1 \\ e^{-i\alpha'} \end{pmatrix} \quad (4)$$

One beam aperture can be described as $A(x, y)$, and the second one as $B(x, y) = e^{i\phi(x,y)}$, representing a relative phase between both beams described by $\phi(x, y)$. As shown in Fig. 1, placing a grating of spatial period $d = \lambda f/x_0$ on the Fourier plane, the corresponding transmittance is given by $G(\mu, \upsilon)$. The image $\vec{O}'(x, y)$ formed by the system consists basically of replications of each beam at distances $X_0$; that is, the convolution of $\vec{O}(x, y)$ with the Fourier transform of the phase grating. Invoking the condition of matching first-neighbouring orders, $X_0 = x_0$, $q' = q + 1$ and $r' = r$, the image

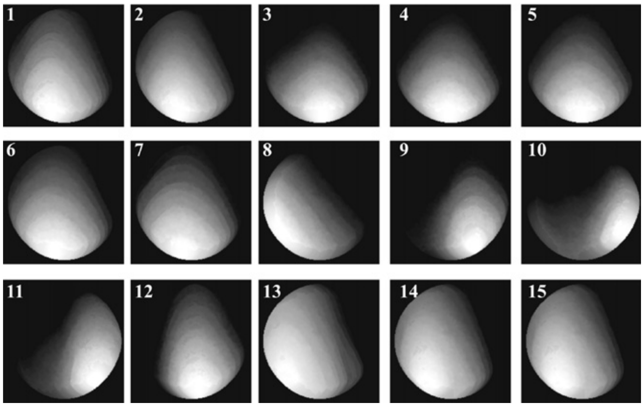


**Fig. 4.** Representative frames. Temporal evolution of the phase profile of the flame. Scale [−1,1] rad.

is then basically described by

$$\begin{aligned}\vec{O}'(x,y) &= \vec{O}(x,y)\otimes\tilde{G}(x,y) = \vec{J}_L\sum_{q,r}^{\infty} J_qJ_r\cdot A(x-(q+1/2)x_0, y-rx_0)\\ &\quad +\vec{J}_R\sum_{q',r'}^{\infty} J_{q'}J_{r'}\cdot B(x-(q'+1/2)x_0, y-r'x_0)\\ &= \sum_{q=-\infty}^{\infty}\sum_{r=-\infty}^{\infty}\{\vec{J}_LJ_qJ_r+\vec{J}_RJ_{q+1}J_r\cdot e^{[i\phi(x-(q+1/2)x_0, y-rx_0)]}\} \end{aligned} \tag{5}$$

After placing a linear polarizing filter at an angle $\psi$ in the transmission axis, its irradiance results as being proportional to

$$\begin{aligned}\left|\left|\vec{J}'_LJ_qJ_r+\vec{J}'_RJ_{q+1}J_re^{i\phi(x',y')}\right|\right|^2 &= A(\psi,\alpha')\cdot[(J_qJ_r)^2+(J_{q+1}J_r)^2\\ &\quad +2J_qJ_r^2J_{q+1}\cdot\cos[\xi(\psi,\alpha')-\phi(x',y')]]\end{aligned} \tag{6}$$

where $x'$ and $y'$ are the coordinates of the image plane,

$$\vec{P}_\psi = \begin{pmatrix}\cos^2\psi & \sin\psi\cos\psi\\ \sin\psi\cos\psi & \sin^2\psi\end{pmatrix}, \quad \vec{J}'_L=\vec{P}_\psi\vec{J}_L, \quad \vec{J}'_R=\vec{P}_\psi\vec{J}_R \tag{7}$$

$A(\psi,\alpha')$ and $\xi(\psi,\alpha')$ are defined as [8]. Fringe contrast $m_{qr}$ is represented by

$$m_{qr}=\frac{2J_qJ_{q+1}}{J_q^2+J_{q+1}^2}, \tag{8}$$

where each fringe contrast depends on the relative phases between the Bessel functions $J_q$.

### 3.1. 2D interference patterns generated by diffraction

The interference patterns are obtained from the interference between the replicas of each beam, centred on each diffraction order. Fig. 2(a) presents the replicas of beam A, with right circular polarization, and the replicas of beam B, with left circular polarization; each order is superposed depending on separation $x_0$ of the beams at the output of the system. Fig. 2(b) presents the interference pattern generated by the interference of contiguous orders [(−1,−2)(0,−1)(+1,0)(+2,+1)], where $x_0$ = 0.8 cm. In order to present one of the principals novelties of the system proposed, interference patterns generated by other diffraction orders are presented.

Fig. 2(c) presents the interference pattern generated by the interference of orders [(−2,0)(−1,+1)(0,+2)] with $x_0$ = 1.8 cm. The anterior results presented allow obtaining interference patterns with the same amplitude and modulation. Out of convenience, the experimental results presented in this work were retrieved through the use of contiguous order interference only, Fig. 2(b).

The experimental observations suggest a simplification for the polarizing filters array due of the phase grid used [2] thus, it is not necessary to use four linear polarizing filters covering four patterns, only two polarizer's need to be placed, each one covering two patterns with complementary phase shifts (See Fig. 2(b)). Then, $\psi_1 = 0°$ and $\psi_2 = 46.577°$, which leads to phase shifts $\xi$ of 0, $\pi$ and $\pi/2$ and $3\pi/2$.

## 4. Experimental results

Due of the use of interference patterns with same amplitude and modulation, scaling and normalization procedure were not necessary, each interferogram obtained was filtered using a low-pass filtering process before phase calculation. The method used for unwrap the phase data was a Quality-Guided Path Following Method [14,15]. For automate the capture and process the phase, we developed a program using Labview 8.5. We are capable of capture one image every 100 ms with a resolution of 480 × 480 pixels. The four interferograms retrieved have relative $\pi/2$ phase shifts generated simultaneously and distributed in a four quadrant image. In order to obtain the optical phase, first a reference phase map is taken, to be subtracted with the phase map of the object in each capture, this is shown in Fig. 3. The four shifted interferograms captured in a shot are shown in Fig. 3(a). The respective phase profile is presented in Fig. 3(b).

Fig. 4 shows the temporal phase evolution for a thin flame candle. These results show that dynamic phase objects can be analyzed with the proposed optical system used [1,13,16].

## 5. Conclusions

The polarizing phase shifting quasi common path interferometer has been described capable of analyse the optical phase data of phase objects. This system is able to obtain several interferograms simultaneously. The combination of grids and conventional polarizing elements optimize the interferometric system, and allows the analysis of static and dynamic objects.

As a proposal of future work, the preliminary results presented of the thin flame suggest the dynamic measurements of temperature fields after a proper characterization, calibration of the optical system and theoretical model.

## Acknowledgements

Authors thank M.A. Ruiz for his contribution in proofreading the manuscript. Enlightening comments and references from anonymous referees are also acknowledged. The experimental results are part of the bilateral projects between Mexico-Chile (CONACYT-CONICYT) and Mexico-Italy (CONACYT-MAE).

Author D.-I Serrano-García (Grant: 227470/31458) is very grateful to CONACyT for the graduate scholarship granted, and expresses sincere appreciation to Geliztle.

Author N.-I. Toto-Arellano expresses sincere appreciation to Luisa, Miguel and Damian for the support provided, and to Sistema Nacional de Investigadores (SNI) for Grant 47446. Partial support from CONACYT and Vicerrectoría de Investigación y Estudios de Posgrado (VIEP) through projects 124145 and 154984 is also acknowledged.

## References


[1] G. Rodríguez-Zurita, C. Meneses-Fabian, N.I. Toto-Arellano, J.F. Vázquez-Castillo, C. Robledo-Sánchez, One-shot phase-shifting phase-grating interferometry with modulation of polarization: case of four interferograms, Opt. Express 16 (2008) 7806–7817.

[2] N.I. Toto-Arellano, G. Rodríguez-Zurita, C. Meneses-Fabian, J.F. Vázquez-Castillo, Phase shifts in the Fourier spectra of phase gratings and phase grids: an application for one-shot phase-shifting interferometry, Opt. Express 16 (2008) 19330–19341.

[3] G. Rodríguez-Zurita, N.I. Toto Arellano, C. Meneses-Fabian, J.F. Vazquez-Castillo, One-shot phase-shifting interferometry: five, seven, and nine interferograms, Opt. Lett. 33 (2008) 2788–2790.

[4] N.I. Toto-Arellano, A. Martínez-García, G. Rodríguez-Zurita, J.A. Rayas-Álvarez, A. Montes-Pérez, Slope measurement of a phase object using a polarizing phase-shifting high-frequency Ronchi grating interferometer, Appl. Opt. 49 (2010) 6402–6408.

[5] H. Zhang Hu, Polarization heterodyne interferometry using a simple rotating analyzer. 1: Theory and error analysis, Appl. Opt. 22 (1983) 2052–2056.

[6] J.P. Liu, T.C. Poon, Two-step-only quadrature phase-shifting digital holography, Opt. Lett. 34 (2009) 250–252.

[7] I. Yamaguchi, T. Zhang, Phase-shifting digital holography, Opt. Lett. 22 (1997) 1268–1270.

[8] I. Yamaguchi, J. Kato, S. Ohta, J. Mizuno, Image formation in phase-shifting digital holography and applications to microscopy, Appl. Opt. 40 (2001) 6177–6186.

[9] S. Nakadate, H. Saito, Fringe scanning speckle-pattern interferometry, Appl. Opt. 24 (1985) 2172–2180.

[10] J.A. Ferrari, E.M. Frins, C.D. Perciante, A new scheme for phase-shifting ESPI using polarized light, Opt. Commun. 202 (2002) 233–237.

[11] J.H. Bruning, D.R. Herriott, J.E. Gallagher, D.P. Rosenfeld, A.D. White, D.J. Brangaccio, Digital wavefront measuring interferometer for testing optical surfaces and lenses, Appl. Opt. 13 (1974) 2693–2703.

[12] M. Novak, J. Millerd, N. Brock, M. North-Morris, J. Hayes, J. Wyant, Analysis of a micropolarizer array-based simultaneous phase-shifting interferometer, Appl. Opt. 44 (2005) 6861–6868.

[13] J.C. Wyant, Dynamic interferometry, Opt. Photon. News 14 (2003) 36–41.

[14] D. Malacara, M. Servin, Z. Malacara, Chapter 4 in Phase Detection Algorithms in Interferogram Analysis for Optical Testing, Marcel Dekker, New York, 1998.

[15] C. Ghiglia, M.D. Pritt, Chapter 6 in Two-dimensional Phase Unwrapping: Theory, Algorithms, and Software, John Wiley and Sons, New York, 1998.

[16] D.I. Serrano-García, N.I. Toto-Arellano, A. Martínez García, et al., Simultaneous phase-shifting cyclic interferometer for generation of lateral and radial shear, Rev. Mex. Fís. 57 (2011) 0255–258.